Carbohydrate Polymers 79 (2010) 1150–1156

Contents lists available at ScienceDirect

Carbohydrate Polymers

journal homepage: www.elsevier.com/locate/carbpol

Synthesis and characterization of new $CaCO_3$/cellulose nanocomposites prepared by controlled hydrolysis of dimethylcarbonate

Carla Vilela [a], Carmen S.R. Freire [a,*], Paula A.A.P. Marques [b], Tito Trindade [a], Carlos Pascoal Neto [a], Pedro Fardim [c]

[a] CICECO and Department of Chemistry, University of Aveiro, Campus de Santiago, 3810-193 Aveiro, Portugal
[b] TEMA-NRD, Mechanical Engineering Department, University of Aveiro, 3810-193 Aveiro, Portugal
[c] Laboratory of Fibre and Cellulose Technology, Åbo Akademi University, Porthansgatan 3, F1-20500 Turku/Åbo, Finland

ARTICLE INFO

Article history:
Received 21 September 2009
Received in revised form 16 October 2009
Accepted 22 October 2009
Available online 25 October 2009

Keywords:
Cellulose fibers
Nanocomposites
Calcium carbonate

ABSTRACT

$CaCO_3$/cellulose nanocomposite materials were prepared by the controlled reaction of $CaCl_2$ with dimethylcarbonate ($(CH_3)_2CO_3$) in alkaline medium in the presence of cellulose fibers. The effect of several reaction parameters, such as reaction time, temperature, fiber mass fraction and extent of cellulose modification (carboxymethylation), on the final properties of the nanocomposites was investigated by ICP-AES, FT-IR, XRD, SEM, TGA, ToF-SIMS and XPS. The results showed that the hydrolysis conditions strongly influenced the quantity and morphology of $CaCO_3$ particles deposited at the surface of cellulosic fibers. Under specific experimental conditions, the substrate promoted the selective control growth of $CaCO_3$ at the surface of the fibers. The use of these $CaCO_3$/cellulose nanocomposites as reinforcing materials in polyethylene (PE) based composites was also tested. Preliminary DMA studies showed a much higher mechanical performance for the composites with the $CaCO_3$/cellulose fibers nanocomposites as compared to cellulose fibers.

1. Introduction

Cellulose is an almost inexhaustible polymeric raw material with outstanding properties (Klemm, Heublein, Fink, & Bohn, 2005). This polysaccharide has been, for many years, an important raw material used in the form of intact wood for construction purposes, natural textile fibers (cotton) and paper. The use of cellulose as a chemical raw material started in the 19th century, with the production of cellulose nitrate (Klemm et al., 2005), and since then, a wide range of new derivatives has been developed and produced in large scale. Cellulose derivatives are currently used in a broad field of applications, such as optical films, coatings, controlled released systems, biodegradable plastics, biomedical materials and composites (Bledzki & Gassan, 1999; Klemm, Philipp, Heinze, Heinze, & Wagenknecht, 1998a).

More recently, particular attention has been devoted to the development of nanocomposites based on cellulose and inorganic nanoparticles, such as SiO_2 (Pinto, Marques, Barros-Timmons, Trindade, & Pascoal Neto, 2008; Sequeira, Evtuguin, Portugal, & Esculcas, 2007), TiO_2 (Marques, Trindade, & Pascoal Neto, 2006), gold (Pinto, Marques, Martins, Pascoal Neto, & Trindade, 2007), kaolin particles (Fahmy & Mobarak, 2008), among others, because these materials show normally improved mechanical, optical and thermal properties due to the combination of inorganic and organic components in the final material. Calcium carbonate is one of the most abundant biominerals as formed in corals, pearls, mollusc shells, egg shells and the exoskeleton of arthropods (Meldrum, 2003; Weiner & Addadi, 1997). Industrially, besides its application as a filler in papermaking, it has been also used as filler in composite materials, such as in plastics, or as an auxiliary pigment in paints and in paper coating dispersions. In such applications, $CaCO_3$ is simply mechanically blended with the other components of the final materials. However, the information regarding hybrid composite materials of cellulose and calcium carbonate where $CaCO_3$ is precipitated in a controlled way on an organic substrate is still very scarce. The main studies deal with the interactions between cellulose fibers and $CaCO_3$ particles (Fimbel & Siffert, 1986), the kinetics of the process of calcite overgrowth on cellulose powder substrate (Dalas, Klepetsanis, & Koutsoukos, 2000), and the co-precipitation of $CaCO_3$ on pulp (Subramanian, Maloney, & Paulapuro, 2005). In this context, the development of new hybrid nanocomposite materials based on the controlled precipitation of $CaCO_3$ on cellulose fibers, could represent an important contribution for traditional industries, as well, as for drawing new potential applications for these raw materials.

The present study reports the synthesis and characterization of $CaCO_3$/cellulose nanocomposites and envisages their use as fillers in reinforced polyethylene based composites. The $CaCO_3$/cellulose

* Corresponding author.
E-mail address: cfreire@ua.pt (C.S.R. Freire).

0144-8617/$ - see front matter © 2009 Elsevier Ltd. All rights reserved.
doi:10.1016/j.carbpol.2009.10.056

nanocomposites were prepared by the *in situ* synthesis of $CaCO_3$ particles in the presence of two cellulose substrates: hardwood bleached kraft pulp and carboxymethylated cellulose fibers.

2. Experimental

2.1. Materials

The wood cellulose fibers used in this study were *Eucalyptus globulus* Elementary Chlorine Free (ECF) bleached kraft pulp supplied by a Portuguese pulp mill. Monochloroacetic acid (⩾99%) and isopropanol (⩾99%) were purchased from Fluka. Calcium chloride anhydrous (93%), dimethylcarbonate (DMC) (99%) and low density polyethylene (LDPE, mp = 116 °C, d = 0.925 g/mL) were purchased from Sigma–Aldrich. Other chemicals and solvents were of laboratory grades and used without further purification.

2.2. Preparation of carboxymethylated cellulose fibers

The controlled carboxymethylation of the cellulose fibers (CMC) was performed by adapting the classic etherification reaction with monochloroacetic acid (Klemm, Philipp, Heinze, Heinze, & Wagenknecht, 1998b). Air-dried cellulose fibers (3 g) were suspended in isopropanol (80 mL) and then 8 mL of NaOH aqueous solution (30 wt.%) were added dropwise during 30 min at room temperature. The mixture was then stirred during 1 h. After this period, monochloroacetic acid (1 g) was added in small portions during 30 min. The mixture was placed on a water bath at 25 °C (CMC I) or 45 °C (CMC II) for 10 min, with constant stirring. Then, the modified fibers were filtered, suspended in ethanol, neutralized with acetic acid, washed several times with ethanol, and finally dried at room temperature. The carboxyl content (mmol/g) of both unmodified (0.10) and carboxymethylated cellulose fibers (0.49 and 0.83 for CMC I and CMC II, respectively) was determined according to the TAPPI Test Method T 237 om-93 (1993).

2.3. Synthesis of $CaCO_3$/cellulose nanocomposites

The synthesis of $CaCO_3$ nanoparticles, in the presence of cellulose fibers, was adapted from the method reported by Faatz, Gröhn, and Wegner (2004), in which the precipitation of $CaCO_3$ takes place as a result of the release of CO_2 by the hydrolysis of dimethylcarbonate (DMC) in alkaline medium. The effect of several reaction parameters on the characteristics of the nanocomposites was investigated. The experimental conditions used in the optimization process to prepare the nanocomposites are listed in Table 1. A typical synthesis of $CaCO_3$/cellulose nanocomposites started with the addition of 111 mg of $CaCl_2$ and 420 μL of DMC to 80 mL of a cellulose-water suspension (0.1% or 1.0% of fiber mass fraction) under constant stirring. The precipitation started after adding 20 mL of NaOH solution (0.5 M) to the reaction medium at temperature and reaction time specified in Table 1. The nanocomposite was removed from the reaction mixture by filtration, washed with acetone and dried at 40 °C. After the optimization of the experimental conditions, the synthesis process was scaled-up (nanocomposites N and O) to the use of 10 g of fiber, 1000 mL of distilled water, 1.4 g of $CaCl_2$, 5.2 mL of DMC and 250 mL of 0.5 M aqueous NaOH in order to produce enough nanocomposite for the preparation of PE-based composites and for further characterization.

2.4. Preparation of polyethylene–$CaCO_3$/cellulose composites

Composites were prepared by compounding LDPE with the cellulose fibers and $CaCO_3$/cellulose fibers nanocomposites (nanocomposite N) in a melting mixer (Brabender W30 EHT – Plastograph EC). The mixing temperature was set at 170 °C. First, LDPE pellets were charged and, after melting, the fibers or the nanocomposites were added. The systems were mixed at 100 rpm during 10 min. Two fiber contents (15% and 30%) were studied. Subsequently, the composites were molded in an injection molding machine (Thermo-Haake Minijet II) for DMA analysis.

Table 1
Experimental conditions used for the preparation of $CaCO_3$/cellulose nanocomposites.

Nanocomposite	Substrate	Time (min)	Temperature (°C)	Fiber mass fraction (%)[a]	Carboxyl content (mmol/g)
A	Cellulose	2.5	25	0.1	0.10
B	Cellulose	3.5	25	0.1	0.10
C	Cellulose	5.0	25	0.1	0.10
D	Cellulose	7.5	25	0.1	0.10
E	Cellulose	3.5	70	0.1	0.10
F	Cellulose	3.5	25	1.0	0.10
G	Cellulose	5.0	25	1.0	0.10
H	CMC I	3.5	25	0.1	0.49
I	CMC I	5.0	25	0.1	0.49
J	CMC II	2.5	25	0.1	0.83
K	CMC II	3.5	25	0.1	0.83
L	CMC II	5.0	25	0.1	0.83
M	CMC II	7.5	25	0.1	0.83
N[b]	Cellulose	3.5	25	1.0	0.10
O[b]	CMC I	3.5	25	1.0	0.49

[a] The fiber mass fraction is the ratio between the mass of fibers and the mass of suspension.
[b] Nanocomposites prepared under scale-up conditions.

2.5. Characterization methods

The calcium content in the nanocomposites was determined by Inductively Coupled Plasma-Atomic Emission Spectrometry (ICP-AES) on a Jobin Yvon 70 plus equipment.

The FT-IR-ATR spectra were taken with a Brücker IFS 55 FT-IR Spectrometer equipped with a single horizontal Golden Gate ATR cell. Their resolution was 8 cm^{-1} after 128 scans.

The X-ray diffraction (XRD) measurements were performed on a Philips X'Pert MPD diffractometer using Cu $K\alpha$ radiation. All samples were gently pressed into pellets using a laboratory press before analysis.

Scanning Electron Microscopy (SEM) micrographs were obtained using a high voltage microscope (HITACHI S4100) operated at 25.0 kV. Samples were previously coated with carbon using an EMITECH K950 coating system.

Secondary ion spectra and images were recorded using a Physical Electronics ToF-SIMS TRIFT II spectrometer using a primary ion beam of $^{69}Ga^+$ liquid metal ion source (LIMS) with 15 kV applied voltage, 600 pA aperture current and a bunched pulsed width of 20 ns was used in positive mode. A raster size of 200 μm × 200 μm and at least three different spots were analyzed on each sample. Surface distribution of calcium ions was obtained with the best spatial resolution using the ion gun operating at 25 kV, 600 pA of aperture current and an unbunched pulse width of 20 ns. Spectra and images were acquired for 8 min with a fluency of $\sim 10^{12}$ ions/cm^2, ensuring static conditions. Charge compensation was performed using an electron flood gun pulsed out of phase with the ion gun.

X-ray photoelectron spectra were obtained with a Physical Electronics PHI Quantum 2000 ESCA instrument equipped with a monochromatic Al $K\alpha$ X-ray source and operated at 25 W, with a combination of electron flood gun and ion bombarding for charge compensation. The photoelectron collection was at 45° in relation

to the sample surface and the spot size was 500 μm × 400 μm. At least three different spots were analyzed on each sample. The pass energy was 187.85 and 23.50 eV for low and high-resolution, respectively. Curve fitting of C1s peak was performed using a Shirley background and the following binding energies, relative to C1 position (C–C, C–H), were employed for the respective groups: 1.7 ± 0.2 eV for C2 (C–O), 3.1 ± 0.3 eV for C3 (O–C–O or C═O), 4.6 ± 0.3 eV for C4 (O═C–O), 5.6 ± 0.3 eV for C5 (CO_3^{2-}), 8.6 ± 0.3 eV for C6 and 10.6 ± 0.3 eV for C7.

Dynamic mechanical analysis (DMA) experiments were carried out in a Tritec 2000 Dynamic Mechanical Analyzer – Triton Technology, at a constant frequency of 1 Hz from −70 to 120 °C at a heating rate of 4 °C/min.

3. Results and discussion

3.1. Synthesis and characterization of $CaCO_3$/cellulose nanocomposites

In order to optimize the precipitation reaction of $CaCO_3$ at the surface of the fibers, a series of $CaCO_3$/cellulose nanocomposites were prepared under distinct experimental conditions (Table 1), namely reaction time, temperature, fiber mass fraction and extent of cellulose carboxymethylation.

The percentage of calcium, and thus the amount of $CaCO_3$, in the cellulose fibers was determined by inductively coupled plasma-atomic emission spectrometry (ICP-AES). According to the results presented in Fig. 1, the amount of $CaCO_3$ present in the cellulose fibers increased with reaction time and with temperature of synthesis. As expected, higher fiber mass fraction in the reacting suspension resulted in much lower percentages of $CaCO_3$. Conversely, the amount of $CaCO_3$ particles in the unmodified cellulose fibers is higher than in the CMC fibers. As will be discussed bellow, this can be explained by the fact that CMC fibers promote the controlled growth of $CaCO_3$ nanoparticles and avoid the precipitation of larger particles or particle aggregates on the fibers as well as on the bulk of the solution. Finally, the percentage of Ca^{2+} is higher for CMC II (carboxyl content: 0.83 mmol/g) than for CMC I (carboxyl content: 0.49 mmol/g), which clearly confirmed that higher carboxyl content promoted the precipitation of higher amounts of $CaCO_3$ particles, as already reported by other researchers (Dousi, Kallitis, Chrissanthopoulos, Mangood, & Dalas, 2003).

The FT-IR spectra of the $CaCO_3$/cellulose fiber nanocomposites (not shown) demonstrated that all the nanocomposites have the typical absorption bands of the cellulose backbone (Klemm et al., 1998a). Moreover, the strong band at 1420 cm^{-1} and medium intensity band at 876 cm^{-1} in the IR spectra provide confirmation for the presence of calcite, the most stable polymorph of $CaCO_3$ (Xyla & Koutsoukos, 1989). The FT-IR results are in agreement with the ICP-AES results. However, we note that in the case of nanocomposite E, the FT-IR spectrum does not show the diagnostic bands for $CaCO_3$ though Ca has been detected by ICP-AES in this nanocomposite (Fig. 1). As will be discussed later, the powder XRD of this sample show the presence of $Ca(OH)_2$.

The degree of crystallinity of the cellulose fibers and the polymorphism of $CaCO_3$ were investigated by XRD (Fig. 2). All the nanocomposites analyzed preserved the XRD pattern of the corresponding cellulosic substrates, suggesting that the deposition of $CaCO_3$ did not modify their ultrastructure. However, the controlled carboxymethylation of the fibers promoted an extensive decrease on the crystalline order of cellulose. With respect to the $CaCO_3$ diffraction patterns, the nanocomposites obtained after a reaction time of 3.5 min (nanocomposite B) are composed by a mixture of two $CaCO_3$ polymorphs: calcite and vaterite, while those obtained for 7.5 min of reaction (nanocomposite D) contain mainly calcite. Although the selective crystallization of $CaCO_3$ polymorphs is a

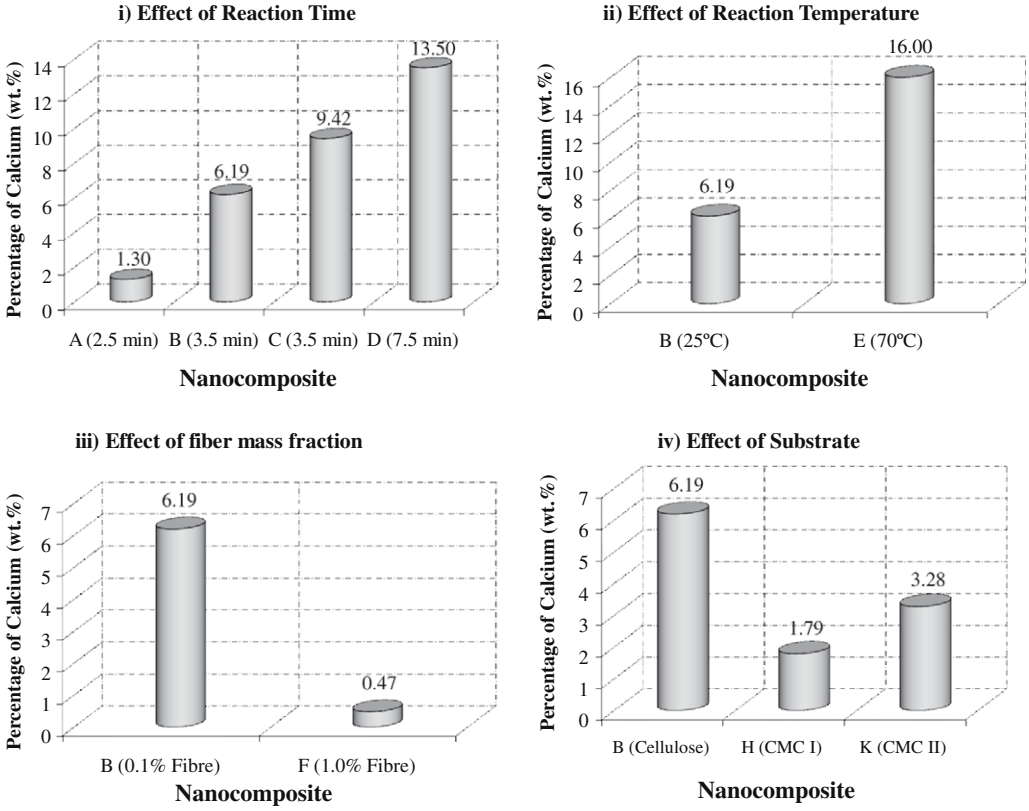

Fig. 1. Effect of some reaction parameters on the final percentage of calcium in the cellulose fibers.

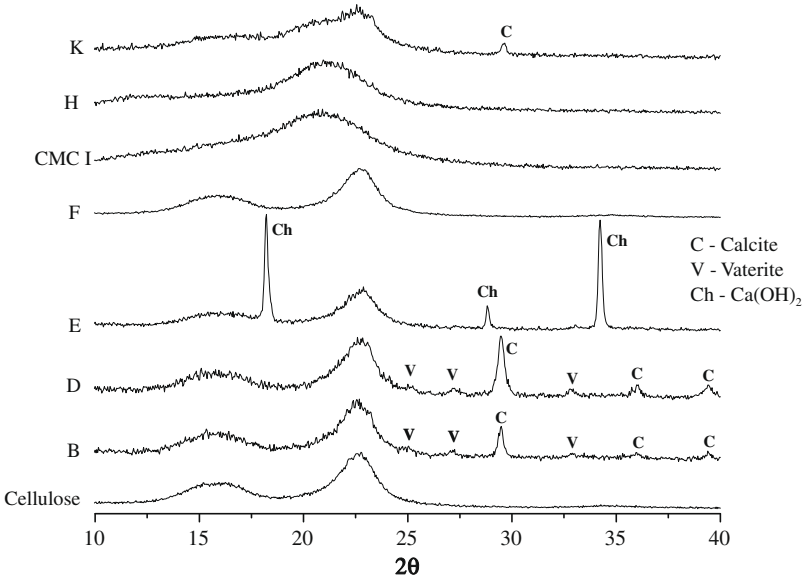

Fig. 2. X-ray diffractogram of cellulose, CMC I and nanocomposites B, D–F, H and K.

rather complex process, involving competitive nucleation and crystal growth of distinct polymorphs, and the phase transformation from metastable to stable forms (Gu, Bousfield, & Tripp, 2006; Kitamura, 2002; Kitamura, Konno, Yasui, & Masuoka, 2002), these results are in agreement with a polymorphic transformation with time of vaterite into the most thermodynamically stable $CaCO_3$ crystalline phase. The nanocomposites obtained at 70 °C (nanocomposite E) exhibited characteristic diffraction peaks of $Ca(OH)_2$ at $2\theta = 18.0°$, 28.7° and 34.1° (Dousi et al., 2003). The absence of $CaCO_3$ in this sample might be related with: (i) the evaporation of dimethylcarbonate, whose boiling point range is 86–89 °C, and thus no subsequent release of a critical amount of CO_2 to promote $CaCO_3$ precipitation; or (ii) a temperature effect on the hydrolysis extent that does not favor the formation of CO_3^{2-}. The XRD pattern of nanocomposites F and H do not show the diffraction peaks of $CaCO_3$ since the amount of calcium carbonate deposited onto the substrate is at a level below the detection limit of this technique. A carboxyl content of 0.83 mmol/g (nanocomposite K) originated a single diffraction peak characteristic of calcite $2\theta = 29.5°$ (Dousi et al., 2003). This indicates that higher contents of carboxyl groups promote the selective precipitation of calcite.

It is worth mentioning that the powder XRD diffractogram (not shown) of $CaCO_3$ particles precipitated by the present method, at 25 °C and for 3.5 min, in the absence of the fibers, only exhibits diffraction peaks assigned to calcite, the most stable polymorph of $CaCO_3$. This suggests that the presence of cellulosic fibers during the precipitation of calcium carbonate influenced its polymorphic form.

The morphological characteristics of $CaCO_3$ particles deposited onto the cellulose fibers were investigated by SEM. The size of the $CaCO_3$ particles ranges between 200 and 700 nm, while the $CaCO_3$ particles shape is predominantly spheroidal for almost every nanocomposites. Fig. 3 shows the SEM micrographs of nanocomposites B, D–F, H and K. The comparison between the SEM images of the nanocomposites B and D shows that increasing reaction times tends to increase the $CaCO_3$ amount in the fibers surface (as previously suggested by ICP-AES) and also tends to increase the size of $CaCO_3$ particles deposited on the cellulose fibers. In addition, the SEM micrograph of nanocomposite B shows that at 25 °C, nanosized (ca. 400 nm) particles with spheroidal morphology were produced, while at 70 °C (nanocomposite E), micrometric aggregates were obtained. When the fiber mass fraction of the reacting suspensions was increased from 0.1% (nanocomposite B) to 1.0% (nanocomposite F) the amount and size of $CaCO_3$ deposited on the fibers diminished, although the morphology of the particles remained spherical. Moreover, it is noteworthy that for 0.1% mass fiber, there is a considerable amount of $CaCO_3$ particles that are not attached into the surface of the fibers, as for example in the case of nanocomposite D (Fig. 3). However, when a higher mass fraction of fiber (1.0%) was used (nanocomposite F) the precipitation of $CaCO_3$ on the bulk of the solution was reduced.

The carboxymethylation of the cellulose fibers (nanocomposites H and K) induced the formation of smaller particles of $CaCO_3$ (ca. 200 nm). Additionally, the use of carboxymethylated cellulose fibers promoted the selective precipitation of $CaCO_3$ on the fiber surface, avoiding the precipitation on the bulk of the solution. Therefore, the increase of carboxyl groups at the cellulose fibers surface promoted the controlled growth of $CaCO_3$, as previously observed with other carboxyl group enriched polymers (Dousi et al., 2003). Although we do not have any clear information about the nature of the interaction of $CaCO_3$ and the cellulosic substrate, it can be suggested that carboxyl groups on CMC may complex Ca^{2+} ions in an initial stage, thus promoting the growth of $CaCO_3$ with lower particle size and homogeneously distributed along the fiber surface.

3.2. Surface characterization of the cellulose fibers: ToF-SIMS and XPS

The ToF-SIMS surface characterization of the nanocomposites N and O clearly confirmed the success of the deposition of calcium carbonate onto the fibers surface, because of the considerable increase of the intensity of peak at $m/z = 40$ attributed to the Ca^{2+} ion (Fig. 4). This increment was higher for nanocomposite O than for nanocomposite N which corroborates the ICP-AES and FT-IR data. Obviously, secondary ions attributed to the fragmentation of the wood pulp fibers backbone, namely, cellulose (127 and 145 Da) and xylans (115 and 133 Da) (Fardim & Durán, 2003), other metal ions and wood extractives (free fatty acid, fatty acid salts and sterols) (Fardim, Gustafsson, Shoultz, Peltonen, & Holmbom, 2005) were also detected in the ToF-SIMS spectra of nanocomposites N and O.

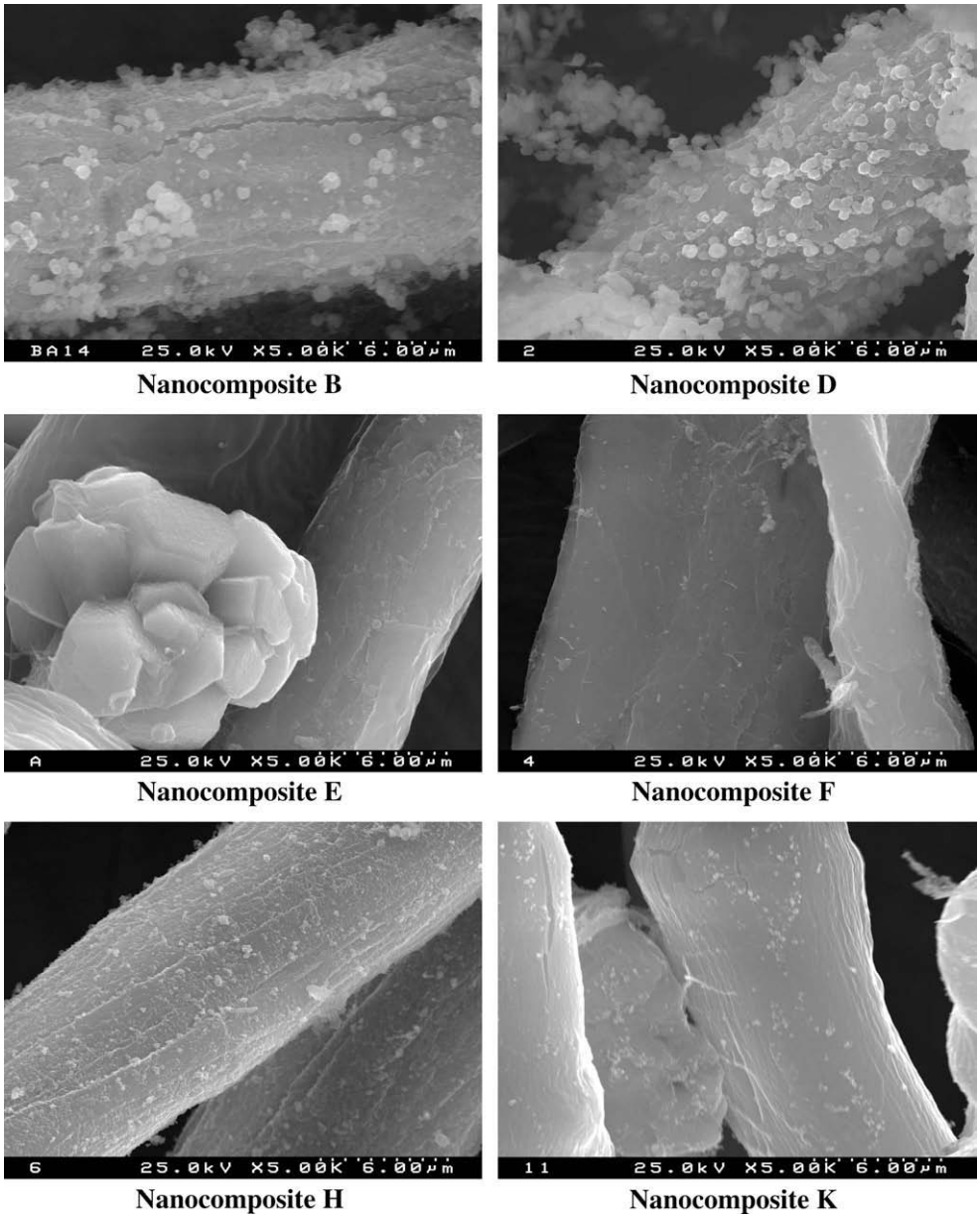

Fig. 3. SEM micrographs of nanocomposites.

The surface chemical composition of the $CaCO_3$/cellulose nanocomposites was also examined by XPS analysis. At low-resolution carbon (~285 eV) and oxygen (~533 eV) (Kroschwitz, 1990) were the dominant elements detected in all samples (Table 2). The presence of $CaCO_3$ was evidenced by the emergence of a peak (Ca2p) at a binding energy of around 350 eV which is characteristic of calcium (Zhang & Gonsalves, 1998). The detection of small amounts of other elements like Na and Cl on the surface of the nanocomposites was related with their ineffective washing during the synthesis procedure. It is worth mentioning that the percentage of calcium present at the surface of nanocomposite N is lower than at the surface of nanocomposite O (Table 2). This higher calcium content is also in agreement with the more pronounced decrease in the carbon content in the surface of nanocomposite O, when compared with the pristine CMC fiber, along with the increase in the oxygen content (in the former composite) resulting from the accumulation of carbonate ions on the fibers surface, both resulting in a marked increase in the O/C ratio. These results corroborate the SEM analysis which indicates that carboxymethylated fibers enhance the selectivity of precipitation on the surface of the fiber, avoiding the precipitation on the bulk of the solution.

The presence of $CaCO_3$ in the surface of the cellulose fibers was also confirmed by the deconvolution of the C1s peak (high-resolution XPS) (Fig. 5) based on the emergence of a peak at around 290 eV assigned to the carbonate carbon atom (CO_3^{2-}) (Gopinath, Hedge, Ramaswamy, & Mahapatra, 2002; Matsushita, Suzuki, Moriga, & Ashida, 1993; Shui, 2003; Wu, He, Chen, Zhang, & Chen, 2006).

Finally, the curve fitting of C1s of nanocomposite N identified two other carbon environments with the binding energies of 8.6 ± 0.3 eV for C6 and 10.6 ± 0.3 eV for C7 relative to the C–C position. These C6 and C7 positions might be assigned to shake-up or plasmon structures rather than emission lines of photoelectron (Gullichsen & Paulapuro, 2000; Kroschwitz, 1990).

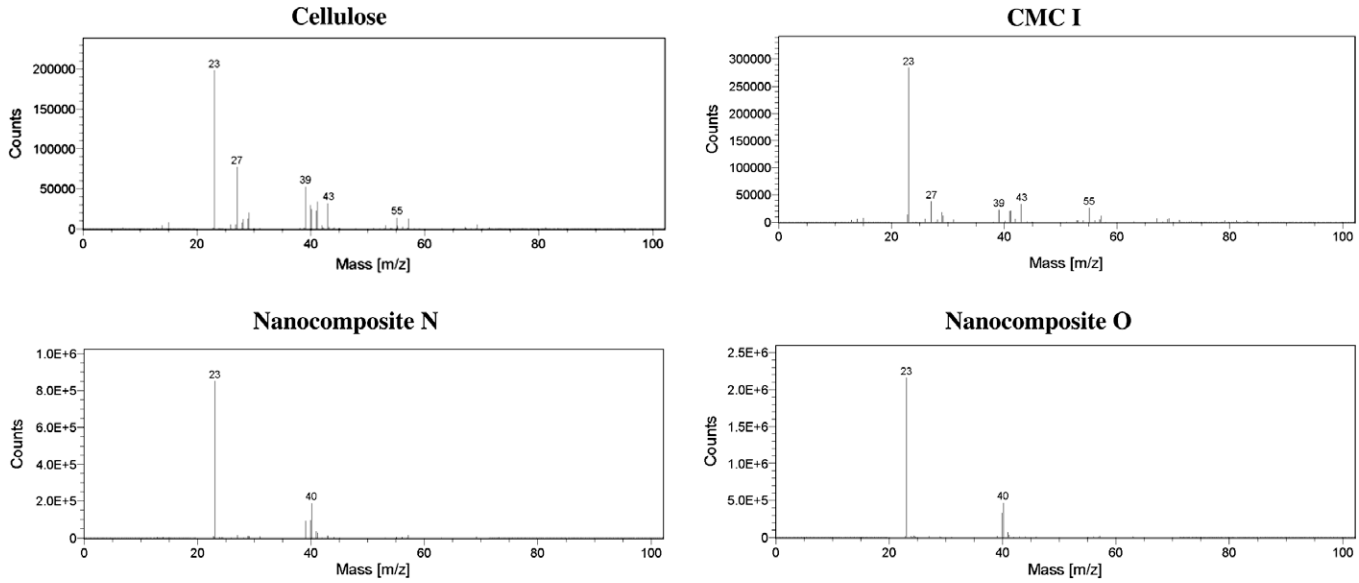

Fig. 4. ToF-SIMS spectra (positive mode) of cellulose, CMC I, nanocomposites N and O.

Table 2
Low-resolution XPS results of cellulose, CMC I, and nanocomposites N and O.

Sample	O (%)	C (%)	O/C	Ca (%)	Na (%)	Cl (%)
Cellulose	42.9	57.1	0.75	–	–	–
Nanocomposite N	42.5	55.1	0.77	2.3	–	0.1
CMC I	35.2	64.2	0.55	–	0.7	–
Nanocomposite O	37.9	51.2	0.74	5.1	5.6	0.2

3.3. Preliminary results of Polyethylene–$CaCO_3$/Cellulose Composites

New polyethylene (PE) based composites were prepared by mixing the polymer with different fillers (cellulose fibers and nanocomposite N) and different filler contents (15 and 30%). The incorporation of cellulose or $CaCO_3$/cellulose (nanocomposite N) as filler in the polyethylene matrix has a significant effect on the storage modulus (E', elastic properties). The DMA analysis showed that the storage modulus of PE and PE-based composites decreased monotonically with the increase in temperature. According to Fig. 6, the E' increased with increasing amount of filler and, for a given percentage of filler, the use of $CaCO_3$/cellulose (nanocomposite N) instead of cellulose originated higher values of storage modulus. This indicates that the presence of $CaCO_3$ particles at the surface of cellulose fibers improved the stiffness of PE-based composites. Thus, the incorporation of $CaCO_3$/cellulose nanocomposite into LDPE demonstrated reinforcement effects which resulted in materials with higher mechanical performance.

4. Conclusions

$CaCO_3$/cellulose nanocomposite materials have been prepared by controlled generation of carbonate in aqueous solution from

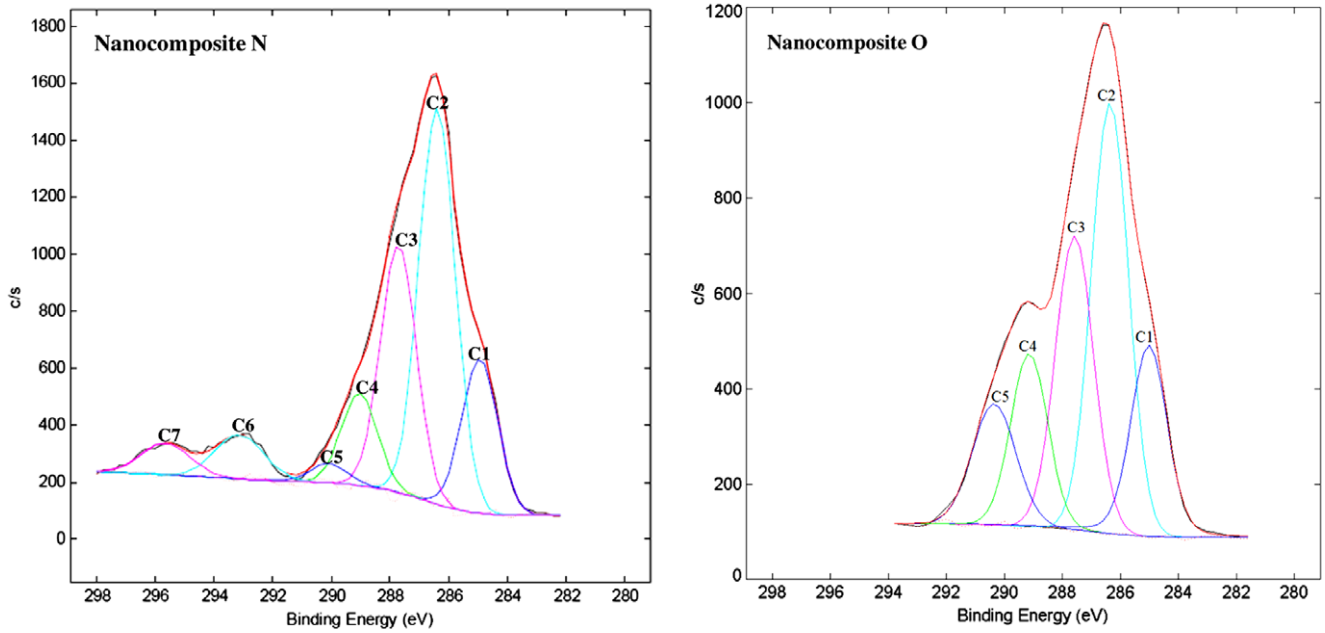

Fig. 5. XPS high-resolution spectra of nanocomposites N and O.

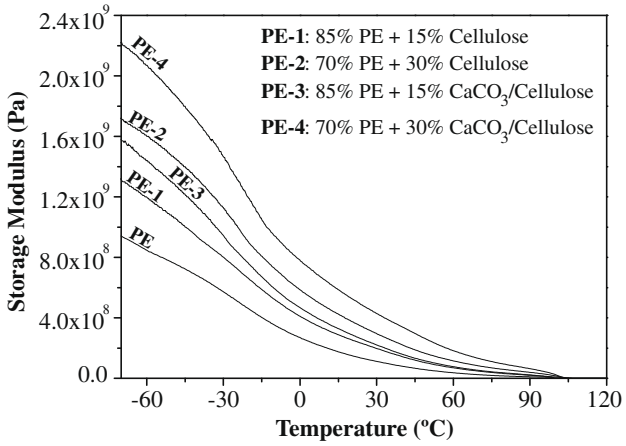

Fig. 6. The dynamic storage modulus curves of PE and PE-based composites.

an organic precursor (DMC) in the presence of cellulose fibers and $CaCl_2$. This work demonstrated that the quantity and morphology of $CaCO_3$ particles deposited at the surface of cellulose fibers were strongly influenced by the hydrolysis conditions. The amount and size of $CaCO_3$ deposited on the cellulose fibers increased with increasing reaction time. Besides, the reactions performed at room temperature originated nanosized $CaCO_3$ particles with spheroid morphology, while at 70 °C micrometric aggregates of $Ca(OH)_2$ were obtained. Additionally, lower mass fractions of fibers in the reacting suspensions favored the formation of spheroid particles of $CaCO_3$. Finally, the presence of carboxyl groups at the substrate surface increased the selectivity of precipitation of $CaCO_3$ particles on the surface of the fibers. The mechanism by which $CaCO_3$ particles are retained at the surface of cellulosic fibers is not understood at this stage, thus it remains an issue that should be further investigated.

$CaCO_3$/cellulose nanocomposites might be considered as potential reinforcing fillers in polyethylene (PE) matrix based composites since preliminary DMA studies demonstrated that PE composites with $CaCO_3$/cellulose fibers showed a much higher mechanical performance.

Acknowledgment

The authors wish to thank the European Commission (SUSTAINPACK IP-500311-2) and Fundação para a Ciência e a Tecnologia (POCI 2010 and REEQ/515/CTM/2005) for the financial support of this work.

References

Bledzki, A. K., & Gassan, J. (1999). Composites reinforced with cellulose based fibres. *Progress in Polymer Science, 24*, 221–274.

Dalas, E., Klepetsanis, P. G., & Koutsoukos, P. G. (2000). Calcium carbonate deposition on cellulose. *Journal of Colloid and Interface Science, 224*, 56–62.

Dousi, E., Kallitis, J., Chrissanthopoulos, A., Mangood, A. H., & Dalas, E. (2003). Calcite overgrowth on carboxylated polymers. *Journal of Crystal Growth, 253*, 496–503.

Faatz, M., Gröhn, F., & Wegner, G. (2004). Amorphous calcium carbonate: Synthesis and potential intermediate in biomineralization. *Advanced Materials, 16*, 996–1000.

Fahmy, T. Y. A., & Mobarak, F. (2008). Nanocomposites from natural cellulose fibres filled with kaolin in presence of sucrose. *Carbohydrate Polymers, 72*, 751–755.

Fardim, P., & Durán, N. (2003). Modification of fibre surfaces during pulping and refining as analysed by SEM, XPS and ToF-SIMS. *Colloids and Surfaces A, 223*, 263–276.

Fardim, P., Gustafsson, J., Shoultz, S., Peltonen, J., & Holmbom, B. (2005). Extractives on fiber surfaces investigated by XPS, ToF-SIMS and AFM. *Colloids and Surfaces A, 255*, 91–103.

Fimbel, P., & Siffert, B. (1986). Interaction of calcium carbonate (calcite) with cellulose fibres in aqueous medium. *Colloids and Surfaces, 20*, 1–16.

Gopinath, C. S., Hedge, S. G., Ramaswamy, A. V., & Mahapatra, S. (2002). Photoemission studies of polymorphic $CaCO_3$ materials. *Materials Research Bulletin, 37*, 1323–1332.

Gu, W., Bousfield, D. W., & Tripp, C. P. (2006). Formation of calcium carbonate particles by direct contact of $Ca(OH)_2$ powders with supercritical CO_2. *Journal of Materials Chemistry, 16*, 3312–3317.

Gullichsen, J., & Paulapuro, H. (2000). *Papermaking science and technology: Forest products chemistry (Book 3)*. Finland: Fapet Oy.

Kitamura, M. (2002). Controlling factor of polymorphism in crystallization process. *Journal of Crystal Growth, 237–239*, 2205–2214.

Kitamura, M., Konno, H., Yasui, A., & Masuoka, H. (2002). Controlling factors and mechanism of reactive crystallization of calcium carbonate polymorphs from calcium hydroxide suspensions. *Journal of Crystal Growth, 236*, 323–332.

Klemm, D., Heublein, B., Fink, H.-P., & Bohn, A. (2005). Cellulose: Fascinating biopolymer and sustainable raw material. *Angewandte Chemie International Edition, 44*, 3358–3393.

Klemm, D., Philipp, B., Heinze, T., Heinze, U., & Wagenknecht, W. (1998a). *Comprehensive cellulose chemistry: Fundamentals and analytical methods* (Vol. 1). Weinheim: Wiley-VCH.

Klemm, D., Philipp, B., Heinze, T., Heinze, U., & Wagenknecht, W. (1998b). *Comprehensive cellulose chemistry: Functionalization of cellulose* (Vol. 2). Weinheim: Wiley-VCH.

Kroschwitz, J. I. (1990). *Polymers: Polymer characterization and analysis*. USA: John Wiley & Sons.

Marques, P. A. A. P., Trindade, T., & Pascoal Neto, C. (2006). Titanium dioxide/cellulose nanocomposites prepared by a controlled hydrolysis method. *Composite Science and Technology, 66*, 1038–1044.

Matsushita, I., Suzuki, T., Moriga, T., & Ashida, T. (1993). XPS study on the carbonation process of $Ca(OH)_2$. *Journal of the Ceramic Society of Japan, 101*, 725–727.

Meldrum, F. C. (2003). Calcium carbonate in biomineralisation and biomimetic chemistry. *International Materials Reviews, 48*, 187–224.

Pinto, R. J. B., Marques, P. A. A. P., Barros-Timmons, A. M., Trindade, T., & Pascoal Neto, C. (2008). Novel SiO_2/cellulose nanocomposites obtained by in situ synthesis and via polyelectrolytes assembly. *Composite Science and Technology, 68*, 1088–1093.

Pinto, R. J. B., Marques, P. A. A. P., Martins, M. A., Pascoal Neto, C., & Trindade, T. (2007). Electrostatic assembly and growth of gold nanoparticles in cellulosic fibres. *Journal of Colloid and Interface Science, 312*, 506–512.

Sequeira, S., Evtuguin, D. V., Portugal, I., & Esculcas, A. P. (2007). Synthesis and characterization of cellulose/silica hybrids obtained by heteropoly acid catalysed sol–gel process. *Materials Science and Engineering C, 27*, 172–179.

Shui, M. (2003). Polymer surface modification and characterization of particulate calcium carbonate fillers. *Applied Surface Science, 220*, 359–366.

Subramanian, R., Maloney, T., & Paulapuro, H. (2005). Calcium carbonate composite fillers. *Tappi Journal, 4*, 23–27.

TAPPI (1993). *TAPPI test methods: T237 om-93 carboxyl content of pulp*. Atlanta: TAPPI Press.

Weiner, S., & Addadi, L. (1997). Design strategies in mineralized biological materials. *Journal of Materials Chemistry, 7*, 689–702.

Wu, W., He, T., Chen, J.-F., Zhang, X., & Chen, Y. (2006). Study on in situ preparation of nano calcium carbonate/PMMA composite particles. *Materials Letters, 60*, 2410–2415.

Xyla, A. G., & Koutsoukos, P. G. (1989). Quantitative analysis of calcium carbonate polymorphs by infrared spectroscopy. *Journal of Chemical Society Faraday Transactions, 1*(85), 3165–3172.

Zhang, S., & Gonsalves, K. E. (1998). Influence of the chitosan surface profile on the nucleation and growth of calcium carbonate films. *Langmuir, 14*, 6761–6766.